Inorg. Chem. **2006**, *45*, 6214–6221

Evaluation of Hexaniobate Nanoscrolls as Support for Immobilization of a Copper Complex Catalyst

Marcos A. Bizeto, Wendel A. Alves, César A. S. Barbosa, Ana M. D. C. Ferreira, and Vera R. L. Constantino*

Departamento de Química Fundamental, Instituto de Química, Universidade de São Paulo, Avenida Lineu Prestes 748, C.P. 26077, CEP 05513-970 São Paulo, Brazil

Received January 11, 2006

In this work, we report the intercalation properties of the hexaniobate nanoscrolls toward insertion of 2-[2-(2-pyridyl)ethylimino-1-ethyl]pyridine-imidazole copper(II), $[Cu(apip)imH]^{2+}$, a cationic complex able to promote the catalytic oxidation of organic substrates. Hexaniobate was first transformed into its acidic phase, $H_2K_2Nb_6O_{17}$, and then exfoliated with *n*-butylamine in water. The copper complex was immobilized into the nanoscrolls obtained by the acidification of delaminated particle dispersion at pH 3. TEM micrographs of particles after immobilization of the cationic complex show scrolls with external diameters of ca. 25–30 nm and wall thicknesses of about 4.5–7.0 nm. The basal spacing (d_{040}) of the copper complex intercalated in hexaniobate is about 11.6 Å. The estimated composition, $[Cu(apip)imH]_{0.5}HK_2Nb_6O_{17}\cdot 6H_2O$, indicates that 50% of the negative charge of interlayer I was neutralized by the copper complex. EPR and IR spectra showed that the ligands and the distorted tetragonal structure of the complex were maintained after immobilization into niobate. The reactivity of this new material toward catechol oxidation using hydrogen peroxide as the oxidizing agent was investigated and compared to the activity of the same complex in solution. The heterogeneous catalyst is initially less effective toward the catechol oxidation but with time, the reaction shows a higher catechol conversion (ca. 82%) than the same copper complex in homogeneous media (ca. 75%). A better reactivity of the heterogeneous catalyst may be related to the stabilization of the immobilized catalyst, preventing its degradation during the reaction course. EPR results show that the kinetics of formation of the DMPO/$^{\bullet}$OH adduct in homogeneous and heterogeneous conditions corresponds to that observed in the catechol oxidation, suggesting that hydroxyl radicals are involved in the reaction mechanism.

1. Introduction

Inorganic layered structures play an important role in the formation of nanocomposites, because they permit the intercalation of different chemical species into the two-dimensional host interlayer regions without disrupting the original structural organization. This characteristic of the layered hosts offers a possibility of designing functional materials by the direct connection among organic, biologic, and inorganic worlds. The host−guest synergism established between the parts may produce new chemical, physical, mechanical, optical, or magnetic properties in the assembled material and offers a wide range of applicability in areas such as heterogeneous catalysis, sensors, nonlinear optics, and others.[1] Our research group has been studying layered niobates as hosts for the intercalation of different kinds of guest molecules, with the aim of preparing new catalysts with peculiar properties. As an example, the structure and semiconducting properties of these materials make them suitable for the development of photocatalysts, especially for water splitting into O_2 and H_2 under UV irradiation.[2]

In this work, we evaluate the use of tubular hexaniobate particles, obtained from the exfoliation of potassium hexaniobate, as supports for transition-metal complexes with catalytic activities. Hexaniobate is built by stacked negative

* To whom correspondence should be addressed. E-mail: vrlconst@iq.usp.br.

(1) (a) Alberti, G.; Costantino, U. In Alberti, G., Bein, T., Eds.; *Solid State Supramolecular Chemistry: Two- and Three-Dimensional Inorganic Networks*; Pergamon: New York, 1996; Vol. 7, p 1. (b) Siegel, R. W., Hu, E., Roco, M. C., Eds.; *WTEC Panel Report on Nanostructure Science and Technology: R & D Status and Trends in Nanoparticles, Nanostructured Materials, and Nanodevices*; Kluwer: Dordrecht, The Netherlands, 1999; Website version: http://www.nano.gov.

(2) Takata, T.; Tanaka, A.; Hara, M.; Kondo, J. N.; Domen, K. *Catal. Today* **1998**, *44*, 17 and references therein.

10.1021/ic0600580 CCC: $33.50
Published on Web 07/12/2006

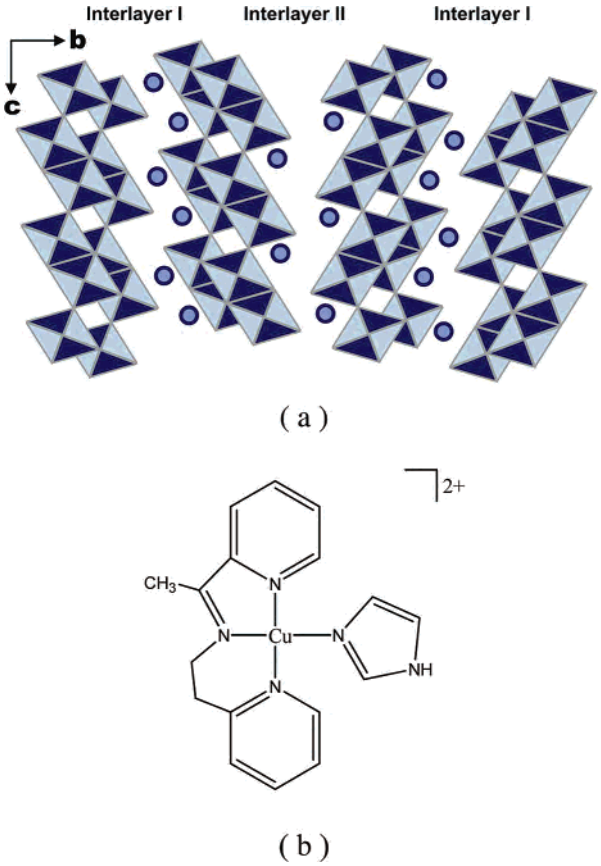

Figure 1. (a) Schematic representation of potassium niobate structure. The distortions in the octahedral units are not shown; (b) $[Cu(apip)imH]^{2+}$ complex structure.

charged layers, and the interlayer region is filled with potassium ions that preserve the charge neutrality. This niobate presents an orthorhombic unit cell containing four layers along the *b*-axis, oriented in such a way that it originates two different interlayer domains (Figure 1).[3] These regions are crystallographically distinct and also show different intercalation properties.[4]

Because of the high layer charge density, the cations are strongly attached to the niobate. Thus, ion exchange reactions, particularly for large species, are very difficult to achieve. By using an appropriate combination of solvent and interlamellar cation, it is possible to promote the niobate exfoliation.[5] The material in the delaminated form can be used to produce new materials with enhanced surface area by promoting sheet restacking in the presence of the desired guest cationic species.[5a−b,6] The exfoliated hexaniobate layers can also be transformed into multiwalled spiral architectures called nanoscrolls. These tubular particles have tunable diameters and are obtained by soft chemical routes on the basis of acidification or an increase in the ionic strength of exfoliated particle dispersion.[5c,7,8] The formation of nanoscrolls is not a particular property of layered niobates. Other lamellar systems such as graphite,[9] WS_2,[10] and titanates[11] are also capable of producing nanoscrolls by analogous processes.

In a recent study,[12] it was shown that the hexaniobate nanoscrolls are capable of intercalate bulky species such as porphyrin, preserving the tubular particle morphology. In the present paper, the intercalation of 2-[2-(2-pyridyl)ethylimino-1-ethyl]pyridine-imidazole copper(II) complex ($[Cu(apip)imH]^{2+}$) (Figure 1b), already described as an oxidation catalyst,[13] into the niobate scrolls is reported. The reactivity of this new material was then investigated through catechol oxidation using hydrogen peroxide as oxidant. Such copper complexes are usually good mimics of copper oxidases,[14] and the niobate structure, similar to the enzyme structure, can promote selectivity and specificity and provide the correct conformation of the substrate in the active site.

The benefits of using the metal complex immobilized on scrolled particles instead of intercalated on the pristine layered niobate are mainly related to the enhancement of the surface area, as shown in previous works on porphyrin intercalation.[6,12] When intercalation was made through the restacking of the exfoliated hexaniobate sheets, the isolated material presented a lamellar arrangement with a surface area of only 8 m^2/g.[6] However, when intercalation was performed using niobate nanoscrolls, the isolated material showed a surface area of about 65 m^2/g.[12] In light of these results, copper-complex-intercalated hexaniobate with a lamellar structure arrangement was not considered in this study. This assumption was also made on the basis of previous studies concerning the reactivity of metal complexes immobilized on layered double hydroxides. It was observed that mainly the species on the basal external surface and edges participate in the catalytic reaction (species located in the interlayer region are not easily accessible to the substrate).[15,16] So, the nanoscroll has a higher external surface area than the pristine layered niobate and also has channels for faster diffusion of the substrate to the active sites. Other advantages to using the scrolled particles are related to the colloidal stability and aggregation features. A dispersion of the scrolled niobate is stable for days, whereas a dispersion of the conventional layered material in the same conditions is stable for only a few minutes. It is also important to remember that hexanio-

(3) Gasperin, M.; Bihan, M. T. L. *J. Solid State Chem.* **1982**, *43*, 346.
(4) Kinomura, N.; Kumada, N.; Muto, F. *J. Chem. Soc., Dalton Trans.* **1985**, *11*, 2349.
(5) (a) Abe, R.; Shinohara, K.; Tanaka, A.; Hara, M.; Kondo, J. N.; Domen, K. *Chem. Mater.* **1997**, *9*, 2179. (b) Abe, R.; Hara, M.; Kondo, J. N.; Domen, K. *J. Mater. Res.* **1998**, *13*, 861. (c) Bizeto, M. A.; Constantino, V. R. L. *Mater. Res. Bull.* **2004**, *39*, 1811.
(6) Bizeto, M. A.; de Faria, D. L. A.; Constantino, V. R. L. *J. Mater. Sci.* **2002**, *37*, 265.
(7) Saupe, G. B.; Waraksa, C. C.; Kim, H. N.; Han, Y. J.; Kaschak, D. M.; Skinner, D. M.; Mallouk, T. E. *Chem. Mater.* **2000**, *12*, 1556.
(8) Du, G.; Chen, Q.; Yu, Y.; Zhang, S.; Zhou, W.; Peng, L. M. *J. Mater. Chem.* **2004**, *14*, 1437.
(9) Viculis, Li. M.; Mack, J. J.; Kaner, R. B. *Science* **2003**, *299*, 1361.
(10) Li, Y. D.; Li, X. L.; He, R. R.; Zhu, J.; Deng, Z. X. *J. Am. Chem. Soc.* **2002**, *124*, 1411.
(11) Ma, R.; Bando, Y.; Sasaki, T. *Chem. Phys. Lett.* **2003**, *380*, 582.
(12) Bizeto, M. A.; Constantino, V. R. L. *Microporous Mesoporous Mater.* **2005**, *83*, 212.
(13) Alves, W. A.; Bagatin, I. A.; Ferreira, A. M. C. *Inorg. Chim. Acta* **2001**, *321*, 11.
(14) Selmeczi, K.; Régheir, M.; Giorgi, M.; Sperier, G. *Coord. Chem. Rev.* **2003**, *245*, 191.
(15) Barbosa, C. A. S.; Dias, P. M.; Ferreira, A. M. C.; Constantino, V. R. L. *Appl. Clay Sci.* **2005**, *28*, 147.
(16) Barbosa, C. A. S.; Ferreira, A. M. C.; Constantino, V. R. L. *Eur. J. Inorg. Chem.* **2005**, 1577.

bate has photocatalytic activity and the nanotube diameter can modify the energy gap.[17] Although photoprocesses are not explored in the present work, modifications in the architecture of the support material (as for example, nanoscroll or stacked layered niobate) can conduct distinct chemical pathways.

2. Experimental Details

2.1. Hexaniobate Synthesis. $K_4Nb_6O_{17}$ was prepared as previously described[5a] by heating a stoichiometric mixture of Nb_2O_5 (CBMM, Companhia Brasileira de Metalurgia e Mineração) and K_2CO_3 (Merck) in a platinum crucible at 1100 °C for 10 h. The crystal structure was confirmed by powder X-ray diffraction (XRD).[18] Potassium hexaniobate was changed to $H_2K_2Nb_6O_{17}$ by refluxing a suspension of $K_4Nb_6O_{17}$ in a 6 mol/L HNO_3 solution for 5 days. The acid solution was replaced after 3 days.[19] The layered structure of $H_2K_2Nb_6O_{17}$ was confirmed by XRD.

2.2. Niobate Exfoliation. The delamination step was carried out as reported previously.[5a] The proton-exchanged niobate (0.5 g) was added to 250 mL of aqueous butylamine solution with an amine: H^+-niobate molar ratio equal to 0.5. The suspension was stirred for 1 week at room temperature. After this period, the flask was kept without stirring for 1 day to allow the separation of the nondelaminated particles (solid fraction deposited in the bottom of the flask) from the dispersion of the exfoliated particles. The deposited solid fraction was rejected and the colloidal dispersion was acidified to around pH 3 with diluted HCl to obtain the tubular particles, as described in the literature.[7] The exfoliated particles were then concentrated by centrifuging the dispersion at 10 000 rpm for 10 min. A material with a gel aspect was obtained and used in the next steps without any further treatment.

2.3. Cu Complex Immobilization. The $[Cu(apip)imH](ClO_4)_2$ complex was synthesized as described in the literature.[13] In its characterization by elemental analysis, the following data were found: C, 36.82; H, 3.45; N, 12.50; Cu, 11.85; very consistent with calculated values considering the formula $C_{17}H_{19}N_5Cl_2O_8Cu$: C, 36.73; H, 3.44; N, 12.60; Cu, 11.43. FTIR and UV−visible spectroscopic data were as follows: ν(OH), 3245 and 3147 cm^{-1} (strong); ν(N−H), 3076 cm^{-1} (medium); ν(C−H), 2973, 2940, and 2870 cm^{-1} (medium); ν(C═N) of Schiff base, 1630 cm^{-1} (strong); ν(C═N) + ν(C═C) of pyridine ring, 1602, 1487, and 1444 cm^{-1} (strong); $\nu_{as}(ClO_4)$, 1094 cm^{-1} (strong). λ_{max} (ϵ, mol^{-1} L cm^{-1}): 200 nm (59.7), 254 nm (17.4), and 282 nm (15.2) for $n \rightarrow \pi$ or $n \rightarrow \pi^*$ transitions, and 624 nm (158) for the d−d band [13] (also see the Supporting Information). Perchlorate salt of metal complexes should be manipulated carefully.

The niobate gel obtained as described above was dispersed in 50 mL of the copper complex aqueous solution containing a 2-fold molar excess of the complex in relation to the proton hexaniobate quantity. The pH of the solution was previously adjusted to 3 with a diluted HCl solution. The system was maintained under stirring at room temperature for 2 days. After this time, the material was recovered by centrifuging, washed with deionized acidified water, and dried in a desiccator with silica gel under a vacuum. The amount of metal complex in the inorganic solid was estimated through thermogravimetric analysis: 8.7 wt % loss from room temperature up to 230 °C; 12.8 wt % at 230−900 °C; calculated loss (considering the formula $[C_{17}H_{19}N_5Cu]_{0.5}HK_2Nb_6O_{17}\cdot 6H_2O$): 9 wt % (water); 13 wt % (12.3% from organic ligands and 0.7% from hexaniobate decomposition). [Cu(apip)imH]-niobate material was also characterized by FTIR and UV−visible electronic spectroscopy, and the following data were found: ν(OH), 3150 cm^{-1} (strong, broad); ν(C═N) of Schiff base, 1643 cm^{-1} (weak); ν(C═N) + ν(C═C) of pyridine ring, 1481 and 1442 cm^{-1} (weak); ν(Nb═O), 902 cm^{-1} (strong). λ_{max}: 263 nm (strong), 292 nm (strong), for $n \rightarrow \pi$ or $n \rightarrow \pi^*$ transitions, and 500−800 nm (strong, very broad), for the d−d band (also see the Supporting Information).

2.4. Sample Characterization. X-ray diffraction (XRD) patterns of powdered samples were recorded on a Rigaku diffractometer Miniflex model using Cu Kα radiation. UV−visible absorption spectra (UV−vis) of the niobate suspensions were recorded in a Shimadzu spectrophotometer model UV-2401PC equipped with an integration sphere. High-resolution transmission electron microscopy (HRTEM) micrographs were recorded on a 300 kV JEM-3010 ARP microscope of the LME/LNLS (Laboratory of Electron Microscopy of the Brazilian Synchrotron Light Laboratory, Campinas, Brazil). Samples were prepared by dispersing the solids in ethanol with an ultrasonic bath followed by deposition on a carbon-coated Cu microgrid. Thermogravimetric analysis (TGA) was performed in a Shimadzu analyzer, model TGA-50, under a synthetic air atmosphere (flow rate = 50 mL/min) using a heating rate of 5 °C/min up to 900 °C. The infrared spectra of solid samples were recorded on a Bomem spectrophotometer, model MB-102, with a reflectance accessory. Samples were diluted in KBr. BET surface area measurements were carried out on a Quantachome analyzer, model Quantasorb, using nitrogen as the adsorbent and helium as the carrier gas. The samples were degassed for at least 3 h at 150 °C. EPR spectra were recorded in Bruker EMX equipment, operating at X-band frequency, using a standard Wilmad quartz tube and DPPH (α,α′-diphenyl-β-picrylhydrazyl) for calibration (g = 2.0036).

2.5. Catechol Oxidation. All reagents used were of commercial grade. Catechol, sodium dihydrogen phosphate, and sodium hydroxide were purchased from Merck. Hydrogen peroxide (30 wt % aqueous solution) was obtained from Fischer Scientific.

Oxidation of catechol was used as a reaction test to evaluate the reactivity of the complex in solution and intercalated in the niobate. The tests were carried out in 8 mL screw-capped glass vials held in a water-jacketed vessel at 30 °C, with the temperature maintained by a thermostated water bath. All solutions were prepared using phosphate-buffered aqueous solution (pH 7). Each experiment was conducted in duplicate, and the copper complex content was the same for both homogeneous and heterogeneous conditions. Catechol conversion was determined indirectly by spectrophotometrically measuring the amount of substrate present after some time intervals during the course of the reaction, using the nitrite method.[20] The catechol derivative was quantified at 510 nm (ϵ_{max} = 10 000 M^{-1} cm^{-1}). To certify that leaching of the copper complex was not taking place under the heterogeneous conditions, we removed and filtered samples at the end of the tests. UV−visible spectra of the filtered solutions do not show the presence of the free complex.

In homogeneous conditions, 1.00 μL of a 5 mM copper complex solution (5 μmol) was added to a glass vial containing 2800 μL of phosphate-buffered solution. Then, 1000 μL of 50 mM catechol (50 μmol) was added followed by 200 μL of 0.875 M H_2O_2 (250 μmol). Under heterogeneous conditions, a similar procedure was used: 4.50 mg of the copper-complex-intercalated niobate (containing 5 μmol of the Cu complex) was suspended in 1920 μL of

(17) Tenne, R.; Rao, C. N. R. *Philos. Trans. R. Soc. London, Ser. A* **2004**, *362*, 2099.
(18) JCPDS file 21-1295; International Center for Diffraction Data: Newtown Square, PA.
(19) Bizeto, M. A.; Constantino, V. R. L. *Mater. Res. Bull.* **2004**, *39*, 1729.
(20) Waite, J. H.; Tanzer, M. L. *Anal. Biochem.* **1981**, *111*, 131.

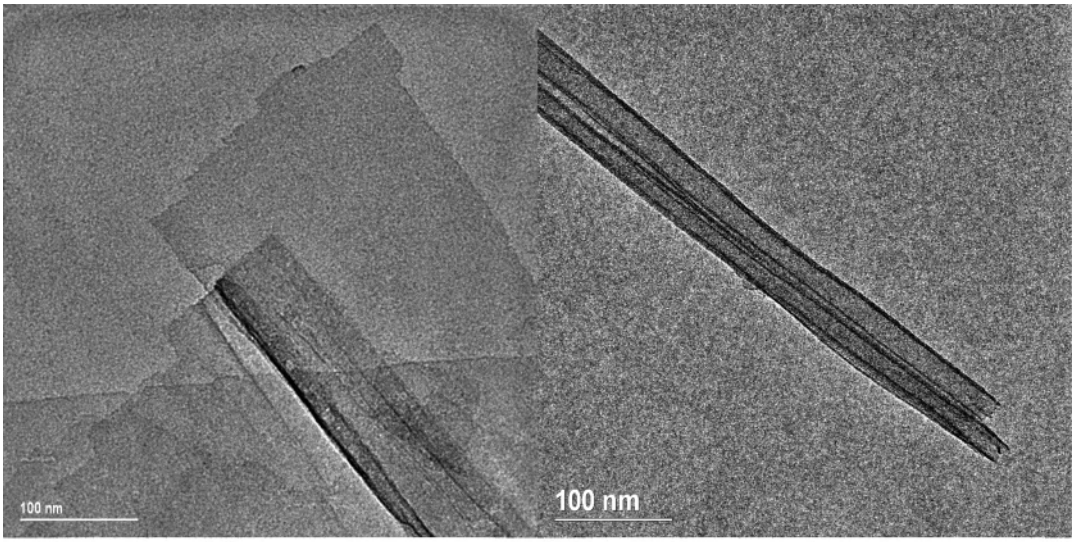

Figure 2. TEM micrographs of exfoliated hexaniobate particles (a) as-synthesized dispersion (pH ~8) and (b) after the acidification of dispersion to pH 3.

phosphate-buffered solution followed by the addition of catechol and hydrogen peroxide solutions. From each reaction vessel, samples were taken at selected time intervals and filtered in a Millipore filter (pore diameter 0.22 μm) before analysis by the nitrite method.

3. Results and Discussions

Most of hexaniobate-exfoliated particles before the pH adjustment have a flat shape, as can be seen in Figure 2a. These particles are composed of a few stacked layers, as they are almost transparent to the microscope beam. When the pH of dispersion is adjusted to values below 7, the flat particles coil into multilayer hollow tubes, as shown in Figure 2b. These tubes do not have a uniform external diameter along the whole particle because of the irregular shape of the exfoliated sheets and the helical angle of rolling that leads to more turns in the inner part than in the end.

The curling mechanism of flat particles to nanoscrolls is not yet well understood. An interesting study has been reported for titanate nanotubes on the basis of TEM and ab initio calculations.[21] The driving force for the curling process seems to be related to the surface tension of the noncentrosymmetric unilamellar sheets that arises from a positive charge deficiency in the surface of the layers.[7,8,21]

Another point yet to be clarified is the possibility of multilayer particles curling, as unilamellar sheets should not be easily formed because of the different intercalation properties of the hexaniobate. Under mild conditions, such as those used to exfoliate the hexaniobate, only interlayer I is reactive, and interlayer II is still filled with potassium ions.[5,19]

The XRD pattern of the material shows 0*k*0 peaks, indicating that the Cu complex is intercalated between the layers that form the tube wall. The basal spacing (d_{040}) of the protonic pristine hexaniobate ($H_2K_2Nb_6O_{17}$) is 8.0 Å.[5]

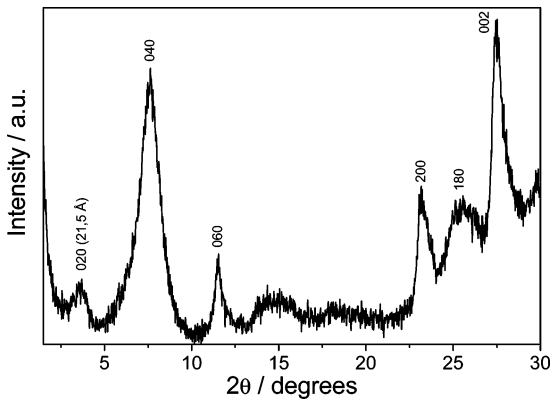

Figure 3. XRD pattern of hexaniobate nanoscrolls intercalated with $[Cu(apip)imH]^{2+}$.

The basal spacing of a *n*-butylamine-intercalated hexaniobate is 12.4 Å.[5] After the copper complex intercalation, the basal spacing of the material is ca. of 11.6 Å, as can be seen in Figure 3. Hence, there is no evidence of *n*-butylamine co-intercalated with the copper complex because all the diffraction peaks related to the layer stacking can be attributed to the same phase.

Considering that all the negative charges of hexaniobate layers are neutralized by the positive charge of the complex and that there is no steric hindrance to achieving this condition, the expected formula for the anhydrous material would be $[C_{17}H_{19}N_5Cu]K_2Nb_6O_{17}$, and the total weight loss in thermogravimetric analysis would be 23.1%. In the registered experimental curve (see the Supporting Information), a first-weight-loss event (ca. 8.7% of the total mass) is observed to occur up to 230 °C, and a second occurs up to 900 °C and corresponds to ca. 12.8% of the total mass. The first event is related to the release of adsorbed water molecules, and the second can be attributed to the decomposition of the organic part of the copper complex, in addition to the hexaniobate dehydroxylation (producing H_2O, Nb_2O_5, and $K_2Nb_4O_{11}$).[19] So, the calculated formula of the material

(21) Zhang, S.; Peng, L.-M.; Chen, Q.; Du, G. H.; Dawson, G.; Zhou, W. Z. *Phys. Rev. Lett.* **2003**, *91*, 256103.

on the basis of TGA experiments is $[Cu(apip)imH]_{0.5}HK_2Nb_6O_{17}\cdot 6H_2O$ (see the Experimental Section). This formula indicates that 50% of the negative charge of interlayer I was neutralized by the copper complex. The total neutralization might not be possible because of the possibility of the copper complex area:charge ratio being greater than the layer charge density of the hexaniobate (12.6 Å^2 per negative charge [22]). TGA data also support the statement that *n*-butylamine is not co-intercalated, because the complex−niobate and butylamine−niobate materials have very different thermal decomposition behaviors.

It is possible to state that the copper complex structure is retained in the niobate scroll on the basis of TGA, XRD, and FTIR data. As was discussed above, the weight-loss percentage obtained by TGA analysis for the material is compatible with the decomposition of the organic ligands. The basal spacing (d_{040}) of the $[Cu(H_2O)_4]^{2+}$-exchanged hexaniobate is 9.37 Å,[23] a low value compared to that observed in Figure 3 (ca. 11.6 Å), suggesting that the copper ion is not intercalated as an aqua complex. The IR vibrational spectrum of the material (see the Experimental Section and the Supporting Information) also indicates that the organic ligands were maintained after the intercalation process. The most evident difference in the IR spectra of the intercalated material compared to that of the free perchlorate complex is the absence of the strong band at 1094 cm^{-1} attributed to the $\nu_{as}(ClO_4)$ vibrational mode. This means that the negative structure of the hexaniobate layers is acting as counterion for the copper complex. Some important bands related to the ν(C═N) and ν(C═C) vibrational modes of the organic ligand rings (about 1490 cm^{-1}) [13] are still present in the FTIR spectrum of the intercalated hexaniobate. It is important to point out that previous works[13,24] have shown that the $[Cu(apip)imH]^{2+}$ complex is very stable toward oxidation by air or aquation reaction. Considering all experimental data described, it is plausible to state that the copper complex identity is maintained after immobilization into niobate nanoscroll.

The reflectance spectrum of the free copper complex and the correlated intercalated hexaniobate are similar (see the Experimental Section and the Supporting Information). The major differences comprise the intensity of the ligand $n \rightarrow \pi$ or $n \rightarrow \pi^*$ transitions in the UV region,[13,24] which are more intense in the intercalated material. The hexaniobate-exfoliated particles present a strong absorption band in the UV region that starts at 330 nm;[5] this band is mixed with the ligand bands, resulting in the observed intensity increase. We also observed in the electronic spectrum of the copper-complex-intercalated material a broadening of the d−d band in the visible region due to changes in the chemical environment around the coordination sphere of the metal into tetragonal geometry. In general, these bands are assigned to the overlapping transitions $d_{xz,yz} \rightarrow d_{x^2-y^2}$ and $d_{xy} \rightarrow d_{x^2-y^2}$.

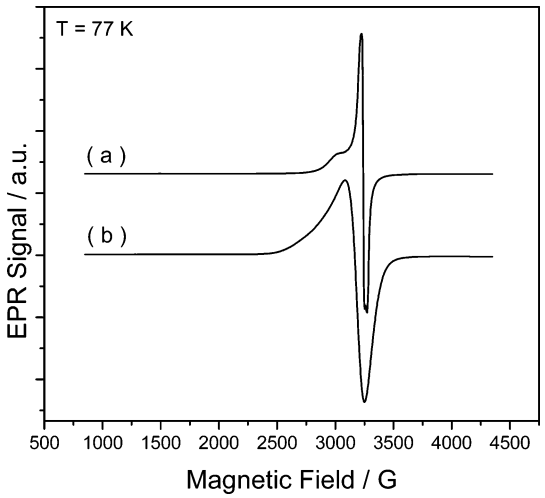

Figure 4. EPR spectra of (a) $[Cu(apip)imH]^{2+}$ (perchlorate salt) and (b) hexaniobate nanoscrolls intercalated with the complex at 77 K.

The energy lowering of $d_{x^2-y^2}$ orbital is observed when the covalent nature of the metal−ligand bond increases, affecting the energy of the $d_{xz,yz,xy} \rightarrow d_{x^2-y^2}$ transition. This fact should be responsible for the difference observed in the λ_{max} of the d−d bands for free and intercalated complex.

The X-band EPR spectra of the free and intercalated copper(II) complex were recorded in the solid state at room temperature, and also at 77 K. The observed spectral profile (Figure 4) shows minor differences between the spectroscopic parameters for the free ($g_{\|} = 2.061$, $g_{\perp} = 2.206$, $g_{iso} = 2.117$) and intercalated complexes ($g_{iso} = 2.108$). The spectrum of the intercalated material shows a broadening of the signals, probably due to intermolecular interactions and the magnetic dipole, but without significant modification on the signal position. The additional peak at 1500 G (near half-field) due to $\Delta M = \pm 2$ transition in dinuclear centers is not observed in the EPR spectra, attesting to the monomeric structure of the copper species in both cases. EPR spectra in the solid state are typical of an axial symmetry with the unpaired electron in the $d_{x^2-y^2}$ orbital, corroborating the UV−vis spectroscopic data.[13,24]

HRTEM micrographs (Figure 5) clearly show the presence of two types of particles: a partially uncoiled and a tubular one. The multilayers that form the tubular particle are easily observed in the edges of the particle (Figure 5b). According to the study performed by Saupe et al.,[7] there is little free-energy difference between the coiled and uncoiled particles, so the process can be reversed. These authors also show that when increasing the pH or decreasing the ionic strength, the tubular particles uncoil. The uncoiling was also observed in suspensions that have been subjected to vigorous stirring, shaking, sonication, or squirting.[7] As sonication was used for the TEM sample preparation, it could have contributed to the partial uncoiling observed in some particles.

The uncoil process can also be related to a great extent of niobate layer charge neutralization by the copper complex. As discussed before, the coil/uncoil process is not yet well understood, and the formation of tubular particles from nanosheets seems to be related to surface strains created by

(22) Gasperin, M.; Bihan, M. T. *J. Solid State Chem.* **1980**, *33*, 83.
(23) Bizeto, M. A.; Christino, F. P.; Tavares, M. F. M.; Constantino, V. R. L. *Quim. Nova* In press.
(24) Alves, W. A.; Azzellini, M. A. A.; Bruns, R. E.; Ferreira, A. M. C. *Int. J. Chem. Kinet.* **2001**, *33*, 472.

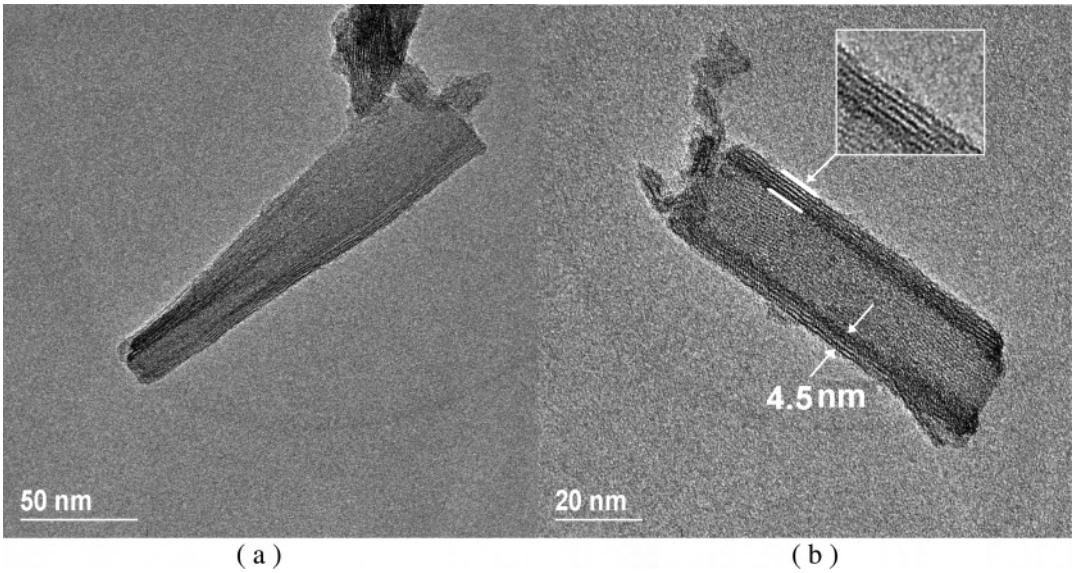

Figure 5. TEM micrographs of the hexaniobate nanoscrolls intercalated with copper complex $[Cu(apip)imH]^{2+}$ showing two different morphologies: (a) partially uncoiled particle and (b) tubular particle.

localized structure distortions, generated by a partial surface-charge neutralization.[7,8,21] So, there is an optimal condition in which the generated surface tension is stronger than the repulsion among the negative layer charges, and this leads to the particle coiling. As the extent of charge neutralization increases, the localized structure distortions are less effective and the surface tension generated is weaker than the particle charge repulsion. This results in the particle uncoiling. The tubular particle shown in Figure 5b has about 5 layers, with a respective wall edge thickness of about 4.5 nm. The external diameter is ca. 25 nm and is very uniform along the whole particle (Figure 5b).

The tubular hexaniobate particles became oriented with the tube axis perpendicular to the view without the use of microtomed samples. Although we did not use any special procedure to prepare oriented samples for TEM images, we observed a particle with the tube axis orientation parallel to the view, as shown in Figure 6. This tube has external and internal diameters of about 30 and 17 nm, respectively. The regular edge thickness of about 7.2 nm indicates that there are eight layers building the wall.

The folding of hexaniobate layers contributed to the enhancement of the surface area. The starting acidic hexaniobate, $H_2K_2Nb_6O_{17}$, has a surface area of 2 m^2/g, whereas the material obtained after the immobilization of the copper complex in the hexaniobate nanoscrolls had its surface area increased to 50 m^2/g.

Dinuclear copper complexes are usually investigated as mimetic systems of tyrosinase or catechol oxidase enzymes,[25] converting phenolic substrates to the related quinones using molecular oxygen as the oxidizing agent. These enzymes have two copper centers coordinated to histidine ligands at the active site, capable of bonding a dioxygen molecule, and thus a wide variety of imidazole-containing ligands have been

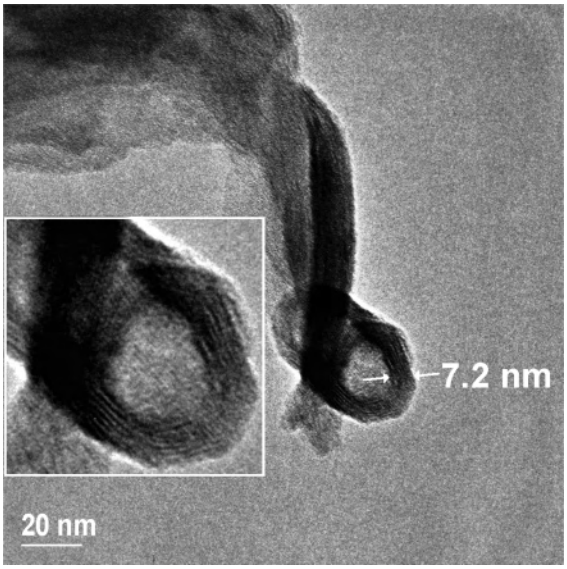

Figure 6. TEM micrographs of a tubular hexaniobate particle intercalated with copper complex $[Cu(apip)imH]^{2+}$; view oriented along the tube axis.

investigated for mimicking structural features of these biomolecules. For $[Cu(apip)imH]^{2+}$, both mono- and corresponding dinuclear species, $[Cu_2(apip)_2im]^{3+}$, coexisted in aqueous solution, exhibiting a pH-dependent monomer−dimer interconversion, with the latter predominating in basic solutions.[14] Although the copper complex was immobilized in the niobate using an acid aqueous solution (pH 3.0), the catechol oxidation experiments were carried out in phosphate-buffered solution (pH 7.0). The main reasons for choosing this pH value are as follows: (i) this copper complex under homogeneous conditions has no appreciable activity in solutions of pH below 7 for the reaction studied in this work; (ii) we can avoid the copper species interconversion during the reaction (the mononuclear is the predominant species at pH 7, as reported previously[14]). Considering that the reactivity experiment was run in phosphate-buffered solution, the hexaniobate should be scrolled in pH 7, because hexaniobate

(25) Duine, J. A.; Jongejan, J. A. In *Bioinorganic Catalysis*; Reedjik, J., Bouwman, E., Eds.; Marcel Dekker: New York, 1999; Chapter 14, p 447.

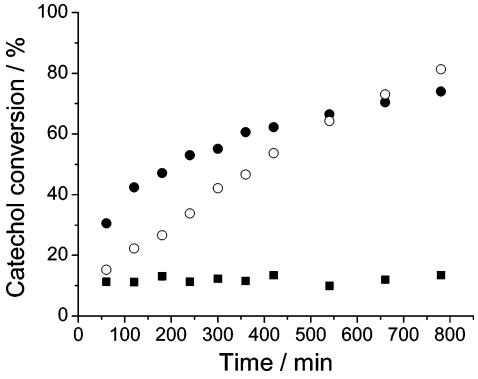

Figure 7. Experimental curves of catechol oxidation using $[Cu(apip)imH]^{2+}$ as catalyst in solution (homogeneous catalyst, full circles) and intercalated in the niobate (heterogeneous catalyst, open circle). Control: noncatalyzed reaction (full squares). Average deviations: ≤5%. Conditions: [catechol] = 10 mM, [CuL] = 1.0 mM, $[H_2O_2]$ = 50 mM.

scrolling is favored by an increase in the ionic strength. The catalytic activity of the Cu complex in the homogeneous phase and immobilized in the niobate nanoscrolls was evaluated toward catechol oxidation, using hydrogen peroxide as the oxidant. The results of catechol conversion are summarized in the curves shown in Figure 7.

The curves of catechol conversion, at 30 °C and pH 7.0, showed negligible reactivity for the system without the copper complex (curves not shown). The reactivity of the copper complex in homogeneous media (Figure 7, solid squares) without hydrogen peroxide (using molecular oxygen from atmospheric air) was low (ca. 10%). In the presence of hydrogen peroxide, the complex converted ca. 75% of catechol after 780 min (Figure 7, full circles). When immobilized in the niobate (heterogeneous catalyst), the material showed higher activity than in the homogeneous phase, converting ca. 82% of substrate (Figure 7, open circles), in the same period of time. Initially, the catechol oxidation was faster using the copper complex in solution rather than using the complex immobilized in the niobate. However, after 540 min, both systems converted nearly the same amount of catechol (ca. 65%). After this time, catechol oxidation is faster in the heterogeneous system. The initial reactivity difference may be explained in terms of substrate diffusion to the active site, which occurs less easily in the heterogeneous than in the homogeneous system.

A better reactivity of the heterogeneous catalyst after some time may be related to the stabilization of the immobilized catalyst, so that it avoids degradation during the reaction course. A similar result has been observed for metal complexes supported and also intercalated on layered double hydroxides.[16]

Although several reaction mechanisms of metal ion species with hydrogen peroxide have been proposed, a paradigmatic one has not yet been established. A mechanism based on the Haber−Weiss reaction or Fenton chemistry assumed that metal ions were utilized through one-electron redox reactions that convert peroxide into reactive radical species.[26] It was

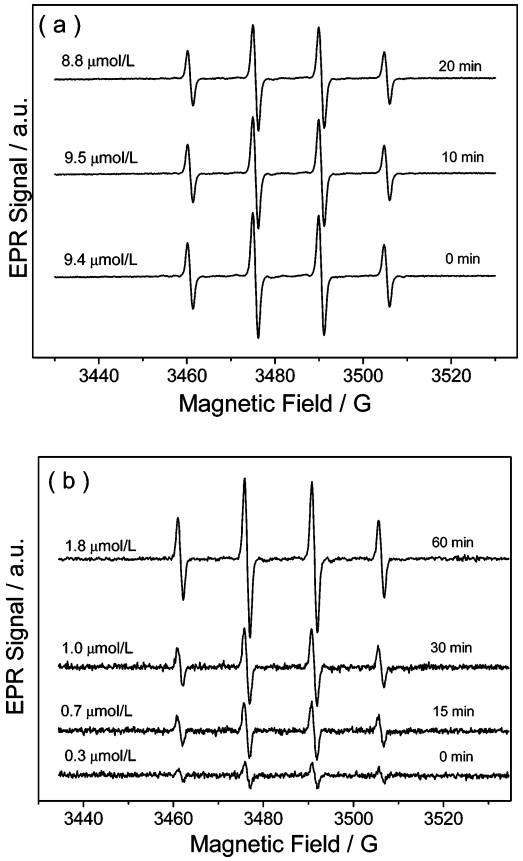

Figure 8. Spectrum of radical adducts generated from a $LCu(II)/H_2O_2$ reaction mixture in the presence of a phosphate buffer solution at pH 7.0 (50 mM). (A) Observed spectrum from a reaction mixture containing 0.25 mM $[Cu(apip)imH]^{2+}$, 5.0 mM H_2O_2, and 100 mM DMPO. (B) Same conditions but using a suspension solution of hexaniobate nanoscrolls intercalated with the complex containing the same concentration of copper (0.25 mM).

claimed that another mechanism included the formation of metal peroxo complexes (MOOH) as the early intermediates, and no radical species were produced.[26b] In this mechanism, the peroxide coordinates to the metal without changing its oxidation state and the substrate might attack the peroxo complex, promoting the activation of the hydrogen peroxide. Commonly, the oxidation reaction is a combination of several mechanisms. To understand the activation mechanism of hydrogen peroxide followed by degradation of target substrates, researchers have developed a number of assays of radical species to distinguish radical chain processes from others.[27]

Therefore, to verify the formation of reactive intermediates in the reaction studied, especially the hydroxyl radical, EPR spectra were taken at both heterogeneous and homogeneous conditions in the absence of catechol, using 5,5′-dimethyl-1-pyrroline-*N*-oxide (DMPO) as the spin trap (Figure 8). However, detection of the DMPO/•OH adduct provides no unambiguous evidence of free hydroxyl radicals trapping. The one-electron oxidation of DMPO by a high-valence metal species, followed by water addition, may also yield

(26) (a) Dunford, H. B. *Coord. Chem. Rev.* **2002**, *233*−*234*, 311. (b) Drago, R. S. *Coord. Chem. Rev.* **1992**, *117*, 185.

(27) (a) Du, Y.; Rabani, J. *J. Phys. Chem. B* **2003**, *107*, 11970. (b) Sun, L.; Bolton, J. R. *J. Phys. Chem.* **1996**, *100*, 4127.

DMPO/•OH formation, as shown below.[28]

$$LCu^{2+} + H_2O_2 \rightarrow LCu^{+} + HO_2^{\bullet} + H^{+}$$

$$LCu^{+} + H_2O_2 \rightarrow LCuO^{+} + H_2O$$

$$LCuO^{+} + DMPO + H^{+} \rightarrow LCu^{2+} + DMPO^{\bullet+} + OH^{-}$$

$$DMPO^{\bullet+} + H_2O \rightarrow DMPO/^{\bullet}OH + H^{+}$$

Particularly, a four-line signal, characteristic of the DMPO/•OH adduct, is observed in EPR spectra for both heterogeneous and homogeneous catalysts (Figure 8). In the case of the free complex in solution, the radical adduct spectrum registered at some time intervals shows no significant changes in its intensities (Figure 8a) up to 20 min of reaction. However, in the case of the complex immobilized in the hexaniobate nanoscrolls, using the same copper concentration as in the homogeneous experiment, the corresponding spectrum presents marked increases in the intensity of the DMPO/•OH adduct signal during the reaction course (Figure 8b), although in much lower total concentration (∼10-fold less). These results show that the kinetics of formation of the DMPO/•OH adduct under homogeneous and heterogeneous conditions correspond to that observed in the catechol oxidation, suggesting that hydroxyl radicals are probably formed in both of these systems.

In light of these findings, the hydroxyl radical is possibly the predominant active species promoting the oxidation of catechol, both in homogeneous and heterogeneous systems. *o*-Quinones are the primary expected oxidation product. However, detailed product identification is complicated because of the possible formation of several products, from quinone to dimer and oligomers. In fact, during the reaction, the formation of a fine black powder was observed. Moreover, further oxidative degradation can lead to aromatic ring cleavage, resulting in other aliphatic products.[29]

Hydrogen peroxide decomposition to water and molecular oxygen (catalase-like activity) during the catechol oxidation reaction was ruled out, because previous studies showed that at pH 7.0 (phosphate-buffered solution), this reaction is neglectful.[18]

Further studies are under development in our laboratory, and the immobilization of di- and tetranuclear imidazolate-bridged copper(II) complexes[30] in the niobate should result in highly active heterogeneous catalysts with tyrosinase-like activity.

4. Conclusions

Exfoliated hexaniobate particles can be coiled into a tubular morphology that preserves the cation-exchange capabilities of the pristine layered niobate. A copper complex was immobilized in the niobate nanostructure and, according to TGA data, nearly half of the negative charges of the niobate layers were neutralized by $[Cu(apip)imH]^{2+}$. Metal species are not only supported on external surfaces of the support but also immobilized between the layers that form the tubular particle walls, as indicated by X-ray diffractometry. TEM micrographs confirm the presence of nanoscrolls and partially uncoiled particles. The material presented an improved catalytic activity toward the catechol oxidation by H_2O_2 in comparison to the catalytic activity of the same complex free in solution. A better reactivity of the heterogeneous catalyst may be related to the stabilization of the immobilized catalyst, which helps it avoid degradation. On the basis of reactivity and EPR results, it is suggested that the hydroxyl radical is the main active species in the catalyzed catechol oxidation.

Acknowledgment. The authors acknowledge the Brazilian agencies FAPESP (Fundação de Amparo à Pesquisa do Estado de São Paulo) and CNPq (Conselho Nacional de Desenvolvimento Científico e Tecnológico) for financial support. We are also thankful to LME-LNLS (Project TEM-2173) for the HRTEM images and to the Companhia Brasileira de Metalurgia e Mineração (CBMM) for the Nb_2O_5 sample.

Supporting Information Available: TGA analysis of hexaniobate nanoscrolls intercalated with $[Cu(apip)imH]^{2+}$. Vibration infrared spectra of hexanobate nanoscrolls intercalated with $[Cu(apip)imH]^{2+}$ compared to the free complex. UV−vis reflectance spectra of hexaniobate nanoscrolls intercalated with $[Cu(apip)imH]^{2+}$ compared to the free complex.

IC0600580

(28) Burkitt, M. J.; Tsang, S. Y.; Tam, S. C.; Bremner, I. *Arch. Biochem. Biophys.* **1995**, *323*, 63.

(29) (a) Meunier, B.; Sorokin, A. *Acc. Chem. Res.* **1997**, *30*, 470. (b) Sorokin, A.; Fraisse, L.; Rabion, A.; Meunier, B. *J. Mol. Catal. A: Chem.* **1997**, *117*, 103.

(30) Alves, W. A.; Almeida-Filho, S. A.; Vieira, M.; Paduan-Filho, A.; Becerra, C. C.; Ferreira, A. M. D. C. *J. Mol. Catal. A: Chem.* **2003**, *198*, 63.